GSA Data Repository 2015054

METHODS DETAILS

Core 64PE-174P13, from the central Walvis Ridge was retrieved ~1800 km northwest from the Agulhas leakage area. We sampled the core in the interval from 112 to 212 cm, at 2 cm resolution, and at 1 cm to obtain higher resolution during the glacial termination II (T-II), based on the stratigraphy of Scussolini and Peeters (2013), to cover most of MIS 6 and 5. Scussolini and Peeters (2013) provided a low resolution time series of $\delta^{18}O$ from *Globigerinoides ruber* and *Globorotalia truncatulinoides* (sinistral). For this study, we increased the resolution of the $\delta^{18}O$ series through the interval of interest, generated Mg/Ca-based temperature reconstructions, and used these time series to reconstruct seawater $\delta^{18}O$ anomaly in the upper water column of the Walvis Ridge. Samples were washed and foraminifera were picked from the 250-300 μm fraction. On average, fifty-five individuals per species were picked, crushed, and subsequently homogenized before splitting into the two aliquots used for $\delta^{18}O$ and Mg/Ca analyses, which were performed at the VU University Amsterdam. We can exclude considerable foraminiferal dissolution in core 64PE-174P13, based on the evidence reported by Scussolini and Peeters (2013) that "shells of delicate juvenile specimens are pristine throughout the core".

Age model

The chronology for core 64PE-174P13 that we use in this study is based on three iterative steps. The “ice-core” timescale for the Agulhas Bank core MD96-2080 of Marino et al. (2013) was converted to a radiometric chronology, using the approach described in Barker et al. (2011). This consisted in applying to the ice core chronology (ECD3, Parrenin et al., 2007) a correction for the offset it manifests with respect to the chronology of radiogenically-dated speleothems (Barker et al., 2011). In the next step, we transferred the absolute chronology to the Walvis Ridge core 64PE-174P13 by graphically correlating its $\delta^{18}O$ *G. ruber* profile to its counterpart from core MD96-2080 (Fig. DR1; Table DR1), which was obtained from the same foraminifer species and morphotype. Finally, we estimated and propagated the different sources of uncertainty (at the 68%, 1σ confidence level) associated with the construction of the chronology for core 64PE-174P13. This error propagation exercise

($\sigma_{chronology}$; Eq. DR1) accounts for: (σ_i) the uncertainties of the MD96-2080 chronology used by Marino et al. (2013); (σ_{ii}) the uncertainties estimated for the conversion of the ice core to the radiometric ages, discussed in Barker et al. (2011); and (σ_{iii}) the temporal resolution (i.e., sample spacing) of the $\delta^{18}O_{G.\ ruber}$ profiles from 64PE-174P13 and MD96-2080:

(Eq. DR1) $$\sigma_{chronology} = \sqrt{(\sigma_i^2 + \sigma_{ii}^2 + \sigma_{iii}^2)}$$

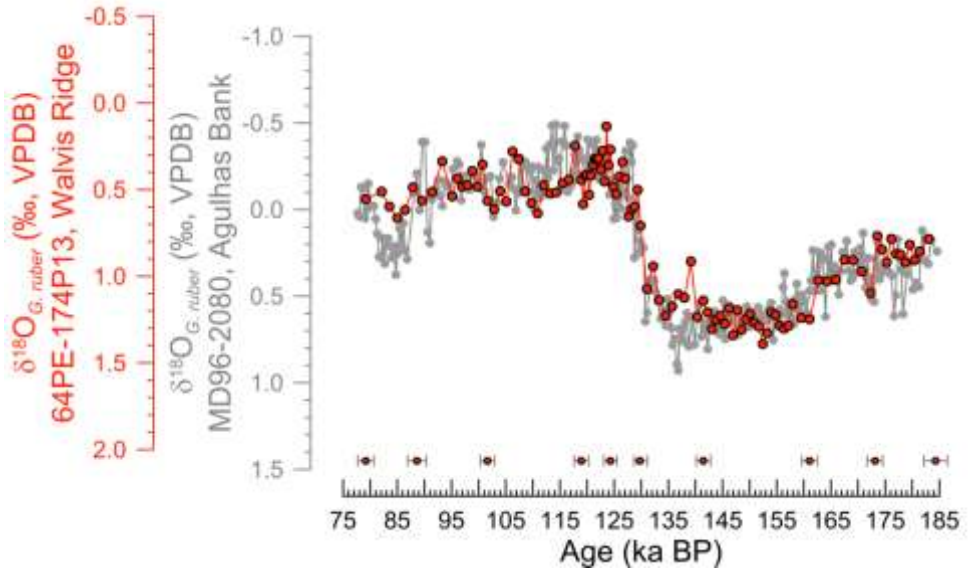

Fig. DR1. **Chronology of core 64PE-174P13**. *G. ruber* $\delta^{18}O$ profile from Walvis Ridge core 64PE-174P13 (red) overlain onto the *G. ruber* $\delta^{18}O$ from Agulhas Bank core MD96-2080. The latter had been previously transferred from an ice core (Marino et al., 2013) to a radiometric chronology, following Barker et al. (2011). The horizontal error bars are the propagated uncertainties at the 68% confidence level (1 σ) associated with the 64PE-174P13 chronology used in this study (see also Table DR1).

Depth 64PE-174P13 (cm)	**MD96-2080 age (ka)**	**Mid-point 64PE-174P13depth (cm)**	**Mid-point age MD96-2080 (ka)**	**±1 σ Uncertainty (k.y.)**
84	77.69	88.0	79.2	1.49
92	80.66			
96	84.72	101.0	88.6	1.73
106	92.54			
114	102.53	115.0	101.7	1.32
116	102.80			

129	118.30	130.0	119.0	1.36
131	119.64			
143	123.65	145.0	124.3	1.23
147	124.98			
151	128.73	155.0	132.8	1.23
159	136.85			
163	140.67	165.0	141.5	1.32
167	142.29			
188	160.49	190.0	161.1	1.44
192	161.67			
204	172.55	205.0	173.2	1.43
206	173.75			
222	180.17	231.0	184.3	2.18
240	188.50			

Table DR1. Age control points for the synchronization of core 64PE-174P13 (central Walvis Ridge) to core MD96-2080 (Agulhas Bank, Marino et al., 2013).

Additionally, we adapted the chronology of core GeoB3603-2 to the one used here by aligning the peak of the Agulhas leakage fauna (Peeters et al., 2004) to the peak in the Agulhas leakage fauna in core MD96-2080 (Martínez-Méndez et al., 2010).

Mg/Ca analysis and temperature reconstructions

Mg/Ca ratios were analysed with a Varian 720 ES inductively-coupled-plasma optical emission spectroscope (de Villiers et al., 2002), after the foraminiferal calcite was cleaned following the procedure outlined in Barker et al. (2003). Briefly, cleaning comprised sonication and rinsing in ultrapure water and methanol, oxidation in hydrogen peroxide, and weak acid leaching. After comparison of the concentration of the remaining potentially contaminant elements on the calcite after cleaning with and without a reductive step, the introduction of such additional reductive step was deemed not necessary. External reproducibility was routinely monitored using standard ECRM 752-1, as recommended by Greaves et al. (2005). The average offset of our measurements on such standard was 0.05 mmol/mol Mg/Ca, from a reported nominal value 3.76 mmol/mol (Greaves et al., 2005), which we corrected for in each run. Intra-run precision was on average ± 0.03 mmol/mol (1σ), corresponding to

0.7%. The following paleotemperature equations were used to convert Mg/Ca values into calcification temperature.

For *G. ruber*, rearranged from Anand et al. (2003):

$$T = \log_n (Mg/Ca / 0.34) / 0.102$$

For *G. truncatulinoides*, rearranged from Regenberg et al. (2009):

$$T = \log_n (Mg/Ca / 1.32) / 0.05$$

Seawater $\delta^{18}O$ anomaly reconstruction

We use paired Mg/Ca-$\delta^{18}O$ time series, in conjunction with contemporaneous records of ice volume changes, to derive local, ice-volume corrected seawater $\delta^{18}O$ ($\delta^{18}O_{sw\text{-}ivc}$) anomalies. First, we correct the $\delta^{18}O$ measured in the foraminiferal calcite ($\delta^{18}O_{foram}$) for the effect of the (calcification) temperature variations. The effect of temperature is estimated from the Mg/Ca composition, using the relationship of Bemis et al. (1998):

(Eq. DR2) $$\delta^{18}O_{seawater} = \delta^{18}O_{foram} - 25.778 + 3.333 \sqrt{(T_{Mg/Ca} + 43.706)}$$

For *G. ruber* we applied a conservative correction of +0.2 ‰ to its $\delta^{18}O$ values, to account for a "vital effect" assessed in situ (Lonçaric et al., 2006). For *G. truncatulinoides* we considered the vital effect negligible (Fairbanks et al., 1980; Loncaric et al., 2006). Subsequently, after converting the VPDB notation to VSMOW, we estimated the $\delta^{18}O_{sw\text{-}ivc}$ by subtracting from the $\delta^{18}O_{seawater}$ the component attributable to variations in mean global seawater $\delta^{18}O$ due to ice-volume variations. For this, we used the recent sea level reconstructions of Grant et al. (2012) for the last 150 ka, and the one of Rohling et al. (2009) for the period 150-183 ka. We converted sea level into mean ocean $\delta^{18}O_{sw}$ using the relationship of Schrag et al. (2002), namely 0.008 ‰ m^{-1}.

Error determination and propagation

The error of the $\delta^{18}O$ measurements was estimated with the pooled standard deviation of replicated measurements. The error on the temperature estimates was propagated from the pooled standard deviation of replicated Mg/Ca measurements, and from the error associated with the "A" and "B" terms of the Mg/Ca temperature calibrations (Anand et al., 2003; Regenberg et al., 2009). The error on the $\delta^{18}O_{sw\text{-}ivc}$ was

propagated from the errors associated with the our Mg/Ca temperature estimation, with our $\delta^{18}O$ measurements, with the sea level reconstructions (Grant et al., 2012), and with the conversion of sea level change into mean $\delta^{18}O_{sw}$ change (Schrag et al., 2002).

Planktic foraminifera calcification depth

Each planktic foraminifer species calcifies along a continuous depth interval (Hemleben et al., 1989). Nevertheless, for convenience of proxy use, a discrete depth is taken to be representative of the average depth of calcification, generally coherent with the geochemical values of the shells collected in the modern water column.

Scussolini and Peeters (2013) assessed apparent calcification depths of *G ruber* and *G. truncatulinoides* sin. in core 64PE-174P13 by comparing core top $\delta^{18}O$ to modern ocean $\delta^{18}O$ of seawater. Therefore for this study we considered that *G. ruber* represented the (sub)surface, and calcified at ~100 m depth, and *G. truncatulinoides* sin. inhabited the thermocline, calcifying around 500 m depth.

ADDITIONAL TABLES AND FIGURES

r and (p) values	64PE-174P13 Surface $\delta^{18}O_{sw\text{-}ivc}$	64PE-174P13 Thermocl. $\delta^{18}O_{sw\text{-}ivc}$	64PE-174P13 Surface Temp.	64PE-174P13 Thermocl Temp.
64PE-174P13 Agulhas rings proxy [1]	**0.79 (p <0.001)**	**0.84 (p <<0.001)**		
MD96-2080 $\delta^{18}O_{sw\text{-}ivc}$ [2]	**0.83 (p <<0.001)**	**0.76 (p <<0.001)**		
MD96-2080 Temp. [2]			**0.55 (p <<0.001)**	0.28 (p < 0.05)

[1] Scussolini et al. (2013)

[2] Marino et al. (2013)

Table DR2. **Correlation statistics between proxy series of core 64PE-174P13 (central Walvis Ridge) and core MD96-2080 (Agulhas Bank)**. Values from core MD96-2080 have been re-sampled at the time step of core 64PE-174P13. Pearson's r correlation coefficients and p significance values are shown. Highly significant correlations are reported in bold.

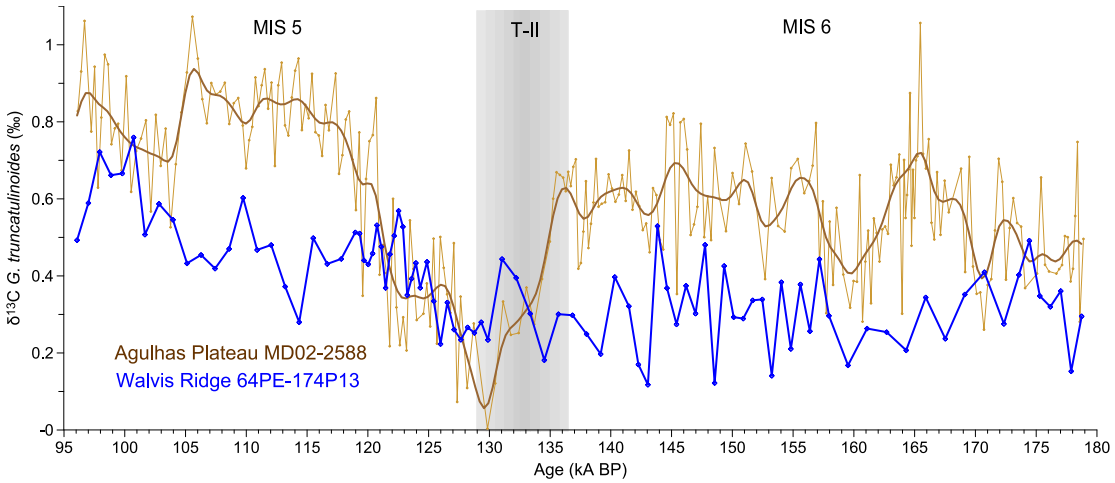

Fig. DR2. **Comparison of thermocline δ^{13}C curves**. We compare the δ^{13}C of *G. truncatulinoides* sin. from Walvis Ridge core 64PE-174-13 (blue) to its counterpart from the Agulhas Plateau core MD02-2588 (brown) (Ziegler et al., 2013; thick line is the result of a 1-k.y. low-pass Gaussian filter). See map in Fig. 1 for reference.

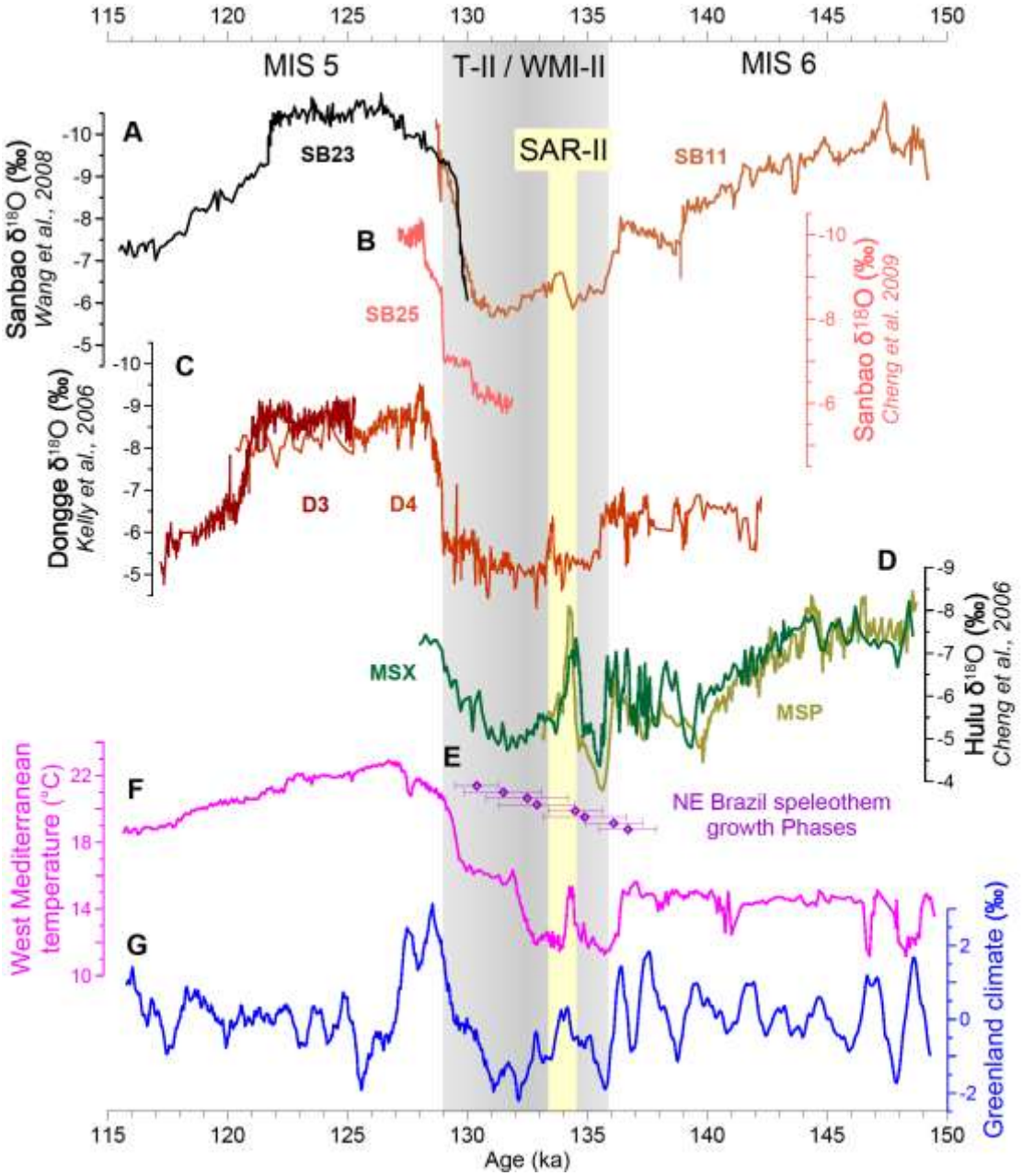

Fig. DR3. **Records from East Asia, Brazil and North Atlantic, displaying climatic evolution at high resolution around T-II, and during the South Atlantic reversal (SAR)-II**. Speleothems A) SB11 and SB23 (Wang et al., 2008) and B) SB25 (Cheng et al., 2009) from the Sanbao cave; C) D3 and D4 from the Dongge cave (Kelly et al., 2006); D) MSX and MSP from the Hulu cave (Cheng et al., 2006). E) Speleothem growth phases from the northeast Brazil caves Lapa dos Brejoes and Toca da Barriguda (Wang et al., 2004). F) Western Mediterranean alkenone-based temperature (Martrat et al., 2014). G) (Synthetic) record of Greenland climate variability (Barker et al., 2011). Records are plotted in their original chronology.

Speleothem	Reference	Midpoint of the event	Age uncertainty
D4	Kelly et al. (2006)	133 ka	± 1.0 k.y.
MSP and MSX	Cheng et al. (2006)	134 ka	± 1.0 k.y.

SB11	Wang et al. (2008)	134 ka	± 1.5 k.y.

Table DR3. **Comparison of timing of the wet interstadial in the weak monsoon interval II**.

DATA OF THIS STUDY

Depth in core (cm)	Age (ka)	*G. ruber* $\delta^{18}O$ (‰)	*G. ruber* temperature (°C)	*G. ruber* $\delta^{18}O_{sw\text{-}ivc}$ (‰)	*G. truncatulinoides* $\delta^{18}O$ (‰)	*G. truncatulinoides* temperature (°C)	*G. truncatulinoides* $\delta^{18}O_{sw\text{-}ivc}$ (‰)	*G. truncatulinoides* $\delta^{13}C$ (‰)
108	95.1	0.539			1.493			0.799
109	96.1	0.436			1.515			0.493
110	97.0	0.483			1.220			0.589
111	97.9	0.475			1.458			0.722
112	98.9	0.393	19.9	1.35	1.284	1.9	-0.68	0.661
113	99.8	0.483			1.343			0.666
114	100.7	0.354	20.3	1.42	1.381	1.9	-0.54	0.760
115	101.7	0.564	20.1	1.57	1.238	2.0	-0.44	0.507
116	102.8	0.614	19.7	1.56	1.440	2.0	-0.28	0.587
117	104.0	0.508	20.4	1.62	1.212	2.2	-0.18	0.546
118	105.1	0.568	19.3	1.44	1.252	2.0	-0.41	0.433
119	106.3	0.281	20.5	1.42	1.283	2.2	0.02	0.454
120	107.4	0.324	19.8	1.31	1.205	1.9	-0.69	0.419
121	108.6	0.511	19.4	1.36	1.341	2.1	-0.20	0.470
122	109.7	0.577	20.7	1.61	1.325	2.0	-0.45	0.603
123	110.9	0.637	20.0	1.60	1.184	2.0	-0.58	0.468
124	112.0	0.474	19.9	1.46	1.489	2.0	-0.29	0.480
125	113.2	0.523	19.3	1.38	1.220	2.1	-0.28	0.372
126	114.4	0.516	20.1	1.56	1.246	2.0	-0.40	0.280
127	115.5	0.463	19.8	1.41	1.362	2.2	-0.06	0.498
128	116.7	0.442	20.7	1.63	1.156	2.0	-0.55	0.431
129	117.8	0.246	20.2	1.36	1.185	2.1	-0.29	0.444
130	119.0	0.444	20.7	1.71	1.306	2.0	-0.38	0.513
131	119.3	0.584	20.0	1.72	1.295	2.0	-0.26	0.510
132	119.7	0.418	19.9	1.54	1.272	2.1	-0.18	0.440
133	120.0	0.411	20.2	1.61	1.207	2.1	-0.15	0.430
134	120.4	0.530	20.3	1.75	1.207	2.1	-0.24	0.458
135	120.8	0.419	20.6	1.73	1.227	2.1	-0.09	0.532
136	121.1	0.358	20.0	1.54	1.416	2.0	-0.18	0.476
137	121.5	0.323	20.5	1.63	1.120	2.1	-0.25	0.369
138	121.8	0.327	20.8	1.69	1.202	2.2	0.10	0.457
139	122.2	0.320	20.3	1.59	1.358	2.2	0.29	0.505

140	122.5	0.386	20.9	1.80	1.142	2.1	-0.21	0.569
141	122.9	0.275	20.8	1.67	1.317	2.2	0.29	0.528
142	123.2	0.453	20.7	1.85	1.176	2.1	-0.02	0.350
143	123.6	0.135	20.9	1.58	1.049	2.3	0.21	0.393
144	124.0	0.361	20.4	1.71	1.169	2.3	0.22	0.434
145	124.3	0.270	20.8	1.70	1.029	2.2	0.01	0.369
146	124.9	0.484	21.4	2.04	1.598	2.1	0.39	0.437
147	125.4	0.526	21.5	2.10	1.366	2.1	0.07	0.334
148	126.0	0.424	21.7	2.06	1.645	2.3	0.73	0.223
149	126.5	0.340	21.5	1.95	1.941	2.2	0.97	0.331
150	127.1	0.435	21.3	2.03	1.445	2.3	0.55	0.261
151	127.7	0.655	21.4	2.29	1.689	2.2	0.72	0.234
152	128.2	0.613	21.5	2.27	1.966	2.1	0.83	0.266
153	128.8	0.598	20.8	2.09	1.821	2.1	0.53	0.252
154	129.3	0.502	20.9	1.99	2.231	1.9	0.61	0.280
155	129.9	0.709	21.3	2.23	1.885	2.0	0.27	0.234
156	131.0	1.072	20.5	2.36	2.202	2.0	0.58	0.444
157	132.2	0.943	20.5	2.12	2.464	2.0	0.74	0.395
158	133.4	1.138	19.6	1.80	2.495	2.0	0.44	0.302
159	134.5	1.227	19.7	1.87	2.278	2.1	0.37	0.181
160	135.7	1.174	19.9	1.85	2.417	2.0	0.42	0.301
161	136.8	1.102	21.4	2.07	2.540	2.0	0.40	0.298
162	138.0	1.124	20.2	1.82	2.527	2.1	0.58	0.249
163	139.2	0.914	20.6	1.64	2.193	2.1	0.16	0.197
164	140.3	1.236	19.3	1.65	2.550	1.9	0.04	0.397
165	141.5	1.140	19.1	1.48	2.468	1.9	-0.09	0.322
166	142.3	1.209	19.4	1.63	2.341	1.8	-0.31	0.170
167	143.1	1.304	19.4	1.73	2.194	1.9	-0.35	0.118
168	143.8	1.250	19.2	1.64	2.481	1.9	0.13	0.529
169	144.6	1.227	19.5	1.70	2.379	1.9	-0.10	0.369
170	145.4	1.276	19.3	1.70	2.266	1.9	-0.23	0.274
171	146.2	1.185	19.0	1.55	2.414	1.9	-0.05	0.375
172	147.0	1.340	19.3	1.79	2.376	1.9	-0.06	0.302
173	147.8	1.195	19.4	1.64	2.543	2.0	0.34	0.481
174	148.5	1.308	19.0	1.68	2.191	2.0	0.00	0.122
175	149.3	1.248	19.6	1.76	2.279	2.0	0.08	0.426
176	150.1	1.216	19.3	1.67	2.088	2.0	0.01	0.293
177	150.9	1.269	19.9	1.83	2.135	2.0	0.00	0.289
178	151.7	1.290	19.3	1.71	2.435	1.9	0.11	0.337
179	152.5	1.390	20.2	2.01	2.118	1.9	-0.24	0.339
180	153.2	1.327	19.6	1.83	2.105	1.9	-0.23	0.141
181	154.0	1.208	20.0	1.79	2.165	1.9	-0.25	0.384
182	154.8	1.224	20.2	1.84	2.098	2.0	-0.04	0.211
183	155.6	1.284	20.2	1.88	2.163	2.0	-0.03	0.378
184	156.4	1.302	20.0	1.85	2.081	1.9	-0.41	0.256
185	157.2	1.288	19.6	1.76	2.286	1.9	-0.10	0.444

186	157.9	1.162	19.4	1.58	2.148	1.8	-0.70	0.297
188	159.5	1.241	19.3	1.58	2.221	1.8	-0.56	0.168
190	161.1	1.248	19.6	1.71	2.217	1.8	-0.52	0.263
192	162.7	1.024	19.3	1.49	2.092	1.8	-0.50	0.254
194	164.3	1.028	19.9	1.66	1.995	1.8	-0.68	0.207

Table DR4. **Results of the geochemical analysis of planktic foraminifera in core 64PE-174P13 (central Walvis Ridge).**

ADDITIONAL REFERENCES CITED

Bemis, B. E., et al. (1998), Reevaluation of the Oxygen Isotopic Composition of Planktonic Foraminifera: Experimental Results and Revised Paleotemperature Equations, *Paleoceanography*, *13*(2), 150-160.

Cheng, H., et al., 2006, A penultimate glacial monsoon record from Hulu Cave and two-phase glacial terminations: Geology, v. 34, p. 217-220.

de Villiers, S., Greaves, M., and Elderfield, H., 2002, An intensity ratio calibration method for the accurate determination of Mg/Ca and Sr/Ca of marine carbonates by ICP-AES: Geochem. Geophys. Geosyst., v. 3, no. 1, p. 1001.

Fairbanks, R. G., Wiebe, P. H., and Bé, A. W. H., 1980, Vertical Distribution and Isotopic Composition of Living Planktonic Foraminifera in the Western North Atlantic: Science, v. 207, no. 4426, p. 61-63.

Grant, K. M., Rohling, E. J., Bar-Matthews, M., Ayalon, A., Medina-Elizalde, M., Ramsey, C. B., Satow, C., and Roberts, A. P., 2012, Rapid coupling between ice volume and polar temperature over the past 150,000 years: Nature, v. 491, no. 7426, p. 744-747.

Greaves, M., et al. (2005), Accuracy, standardization, and interlaboratory calibration standards for foraminiferal Mg/Ca thermometry, Geochem. Geophys. Geosyst., 6(2), Q02D13.

Hemleben, C., M. Spindler, and O. R. Anderson, 1989, Modern Planktonic Foraminifera, Berlin, Springer Verlag, 363 p.

Kelly, M. J., et al. (2006), High resolution characterization of the Asian Monsoon between 146,000 and 99,000 years B.P. from Dongge Cave, China and global correlation of events surrounding Termination II, Palaeogeography, Palaeoclimatology, Palaeoecology, 236(1-2), 20-38.

Lonçaric, N., Peeters, F.J.C., Kroon, D., and Brummer, G.-J.A., 2006, Oxygen isotope ecology of recent planktic foraminifera at the central Walvis Ridge (SE Atlantic): Paleoceanography, v. 21, p. PA3009.

Martrat, B., Jimenez-Amat, P., Zahn, R., and Grimalt, J. O., 2014, Similarities and dissimilarities between the last two deglaciations and interglaciations in the North Atlantic region: Quaternary Science Reviews, v. 99, no. 0, p. 122-134.

Martínez-Méndez, G., Zahn, R., Hall, I.R., Peeters, F.J.C., Pena, L.D., Cacho, I., and Negre, C., 2010, Contrasting multiproxy reconstructions of surface ocean hydrography in the Agulhas Corridor and implications for the Agulhas Leakage during the last 345,000 years: Paleoceanography, v. 25, p. PA4227.

Parrenin, F., Barnola, J.M., Beer, J., Blunier, T., Castellano, E., Chappellaz, J., Dreyfus, G., Fischer, H., Fujita, S., Jouzel, J., Kawamura, K., Lemieux-Dudon, B., Loulergue, L., Masson-Delmotte, V., Narcisi, B., Petit, J.R., Raisbeck, G., Raynaud, D., Ruth, U., Schwander, J., Severi, M., Spahni, R., Steffensen, J.P., Svensson, A., Udisti, R., Waelbroeck, C., and Wolff, E., 2007, The EDC3 chronology for the EPICA Dome C ice core: Clim. Past, v. 3, p. 485-497.

Rohling, E. J., Grant, K., Bolshaw, M., Roberts, A. P., Siddall, M., Hemleben, C., and Kucera, M., 2009, Antarctic temperature and global sea level closely coupled over the past five glacial cycles: Nature Geosci, v. 2, p. 500 - 504.

Schrag, D. P., Adkins, J. F., McIntyre, K., Alexander, J. L., Hodell, D. A., Charles, C. D., and McManus, J. F., 2002, The oxygen isotopic composition of seawater during the Last Glacial Maximum: Quaternary Science Reviews, v. 21, no. 1-3, p. 331-342.